Electronic Supplementary Material (ESI) for Journal of Materials Chemistry A.
This journal is © The Royal Society of Chemistry 2019

Supporting Information

General Self-assembly of Metal/Metal Chalcogenide Heterostructures Initiated by Surface Linker: Modulating Tunable Charge Flow Toward Versatile Photoredox Catalysis

Tao Li, [a] Ming-Hui Huang, [a] Yu-Bing Li, [a] Xiao-Cheng Dai, [a] Yunhui He, [b] Guangcan Xiao, [b] Fang-Xing Xiao [a]*

a. College of Materials Science and Engineering, Fuzhou University, New Campus, Minhou, Fujian Province 350108, China.

b. Instrumental Measurement and Analysis Center, Fuzhou University, Fuzhou, 350002, People's Republic of China.

E-mail: fxxiao@fzu.edu.cn

Table of Contents

Page No.

Experimental details

1. Preparation of one-dimensional (1D) transition metal chalcogenides (TMC)

1.1 CdS nanowires (NWs).[S1] 1.124 g of cadmium diethyldithiocarbamate [$Cd(S_2CNEt_2)_2$], prepared by precipitation from a stoichiometric mixture of sodium diethyldithiocarbamate trihydrate and cadmium chloride in DI H_2O, was added into a Teflon-lined stainless steel autoclave with a capacity of 50 mL. Then, the autoclave was filled with 40 mL of ethylenediamine to 80% of the total volume. The autoclave was maintained at 453 K for 24 h and then allowed to cool to room temperature. A yellowish precipitate was collected, washed with absolute ethanol and DI H_2O to remove residue of organic solvents. The final products were dried in an oven at 333 K for 12 h.

1.2 $Zn_xCd_{1-x}S$ nanorods (NRs).[S2] $ZnCl_2$ and $CdCl_2 \cdot 2.5H_2O$ with different molar ratios were put into Teflon-lined stainless-steel autoclaves together with appropriate amount of $(NH_4)_2S$. Then the autoclaves were filled with 20 wt% ethylenediamine aqueous solution up to 80% of the capacity (50 mL). The autoclaves were maintained at 180 ◦C for 48 h and then cooled down naturally to room temperature. The precipitates were filtered and washed with DI H_2O and ethanol successively. The final products were dried in vacuum at 80 ◦C for 2 h.

1.3 Preparation of $ZnIn_2S_4$ nanotubes (NTs).[S3] In a typical synthesis of $ZnIn_2S_4$ nanotubes, $ZnSO_4 \cdot 7H_2O$ (0.25 mmol), $InCl_3 \cdot 4H_2O$ (0.5 mmol), and TAA (2 mmol) were loaded into a 25 mL Teflon-lined autoclave, which was then filled with 12 mL of pyridine. After 1 h of magnetic stirring, the autoclave was sealed and maintained at 180 °C for 16 h and then allowed to cool to room temperature naturally. The yellow product was collected by centrifugation, washed several times with absolute ethanol and DI H_2O, and finally dried in a vacuum at 60 °C for 4 h.

1.4 Preparation of $CdIn_2S_4$ nanorods (NRs).[S4] *(a) Preparation of CdS nanorods.* Appropriate amounts of analytical grade $CdCl_2 \cdot 2.5H_2O$ and thiourea (Tu) were added to a Teflon-lined stainless-steel autoclave with a capacity of 50 mL, which was filled with ethylenediamine up to 90% of the capacity. The autoclave was maintained at 100-180 °C for 12 h and then air-cooled to room temperature. The precipitate was filtered off and washed with DI H_2O and absolute ethanol to remove residual impurities. After being dried in a vacuum at 70 °C for 3 h, the collected products were characterized to be CdS nanorods. *(b) Preparation of $CdIn_2S_4$ nanorods.* The as-prepared CdS nanorods and $InCl_3 \cdot 4H_2O$ in a molar ratio of 1:2 and excess Tu were also put into an autoclave, which was filled with DI H_2O up to 90% of the total volume. The autoclave was kept at 180 °C for 10 h, and the other procedures are similar to those used for the preparation of CdS nanorods. Finally, orange-yellow powder was obtained for further use.

2. Preparation of MAA-modified TMC (TMC@MAA) nanocomposites

0.1 g of TMC was first dispersed in 100 mL of DI H_2O by sonication for 30 min. Then, 9 mL of 1.0 mol L^{-1} mercaptoacetic acid (MAA) was added under vigorous stirring to facilitate adsorption of MAA on the TMC with MAA for 2 h at room temperature. Finally, MAA-modified TMC were sufficiently rinsed with ethanol to wash away any remaining MAA moiety and finally dried at 333 K in an oven.

3. Preparation of DMAP-capped Au NPs (Au@DMAP NPs)

Synthesis of Au@DMAP NPs was referred to a previously published method.[S5] Prior to experiment, all glassware was cleaned thoroughly with aqua regia (3:1 in volume for HCl and HNO_3) for 12 h and thoroughly washed with DI H_2O. 30 mM aqueous $HAuCl_4 \cdot 3H_2O$ solution (30 mL) was added to 25 mM TOAB solution in toluene (80 mL). The transfer of the gold salt to the toluene phase can be seen within a few seconds. A freshly prepared 0.4 M $NaBH_4$ (25 mL) aqueous solution was added to the above mixture under vigorous stirring, which caused an immediate color change from light yellow to dark red. After 30 min the two phases were separated and the toluene phase was subsequently washed with 0.1 M H_2SO_4, 0.1 M NaOH, and DI H_2O for three times, and then dried with anhydrous Na_2SO_4. Afterwards, an aqueous 0.1 M 4-dimethylaminopyridine (DMAP) aqueous solution (80 mL) was added to aliquots (80 mL) of the as-prepared nanoparticle mixtures. Direct phase transfer across the organic/aqueous interface completed within 2 h with no stirring or agitation required. Finally, Au-dissolved water phase was separated by a separatory funnel and Au@DMAP NPs aqueous solution was thus obtained.

4. Preparation of Au-TMC heterostructures

Au-TMC heterostructures were fabricated by a facile yet efficient electrostatic self-assembly strategy. Specifically, positively charged Au@DMAP NPs aqueous solution (2.2 mg mL^{-1}) was added dropwise into the negatively charged TMC@MAA aqueous dispersion at the weight ratio of 0.005:1, 0.01:1 and 0.02:1 under vigorous stirring. After mixing for 2 h, the mixture was centrifuged and dried in an oven at 333 K.

5. Preparation of Au-CdS NWs (PSS) heterostructure

0.1 g of CdS NWs was dispersed in 100 mL of DI H_2O by sonication for 30 mins, in which 9 mL of 92 mg mL^{-1} polyelectrolyte of poly (sodium 4-styrenesulfonate) (PSS) containing 0.5 M NaCl was added under vigorous stirring for 2 h at room temperature. Subsequently, PSS-modified CdS NWs (CdS@PSS NWs) were sufficiently rinsed with ethanol to wash away any remaining PSS moiety and dried at 333 K in an oven. Au-CdS NWs (PSS) heterostructure was prepared by an electrostatic self-assembly method. Specifically, 4.54 mL of Au@DMAP NPs aqueous solution (0.22 mg mL^{-1}, pH=10) were added dropwise into PSS-modified CdS NWs aqueous solution (1 mg mL^{-1}, pH=10) under vigorous stirring for 2 h to trigger the spontaneous self-

assembly. Finally, the mixture was centrifuged and dried in an oven at 333 K.

6. Preparation of citrated-capped Au NPs (Au@citrate NPs)

Au@citrate NPs were prepared by Dotzauer's method.[S6] In brief, all glassware was thoroughly cleaned with aqua regia for 12 h and rinsed with DI H_2O. In a 100 mL Erlenmeyer flask, 25 mL of aqueous 1 mM $HAuCl_4 \cdot 3H_2O$ was heated to a rolling boil under vigorous stirring (2500 rpm). Aqueous sodium citrate (2.5 mL, 38.8 mM) was also heated to a rolling boil and rapidly added to the above gold precursor solution. After 20 s, the mixture became dark and then burgundy; heating was continued with vigorous stirring for 10 mins. Finally, the mixture was stirred without heating for an additional 15 mins to fulfill the synthesis. The as-prepared Au NPs were stored in a refrigerator at 4 °C in a dark area and used within 2 weeks.

7. Preparation of Au@citrate-CdS NWs heterostructure

Specifically, negatively charged Au@citrate NPs aqueous solution was added dropwise to the negatively charged CdS@MAA NWs aqueous dispersion at the weight ratio of 0.01:1 under vigorous stirring. After mixing for 2 h, the mixture was centrifuged and dried in an oven at 333 K.

8. Preparation of DMAP-capped Pd NPs (Pd@DMAP)

Preparation of Pd@DMAP is analogous to Au@DMAP NPs other than replacing the $HAuCl_4$ precursor with Na_2PdCl_4 under the same conditions.

9. Preparation of Pd-TMC heterostructures

Preparation of Pd-TMC heterostructures is analogous to Au-TMC other than replacing the Au@DMAP NPs with Pd@DMAP under the same conditions.

10. Synthesis of 1.0% Au-CdS NWs nanocomposite by photoreduction method

30 mL of deionized water, 50 mL of methanol and 50 μL of $HAuCl_4$ (40 mg/mL) were mixed together and bubbled with N_2 for 30 min in the dark. 100 mg of CdS NWs was then immersed in the above solution and irradiated with simulated solar light for 60 min by using a 300 W Xe arc lamp (PLS-SXE 300, Beijing Perfectlight). The as-prepared 1.0% Au-CdS NWs was washed with deionized water and dried in an oven overnight at 333 K for 12 h.

11. Synthesis of 1.0% Au-CdS NWs nanocomposite by wet impregnation method

Typical, 100 mg of CdS NWs was dispersed in deionized water by sonication. Then, 10 mL of an aqueous solution containing Au@DMAP NPs with a desirable concentration (0.1 mg/mL) was added using a pipette under vigorous magnetic stirring. After being kept at room temperature for 24 h, the 1.0% Au-CdS NWs nanocomposite were isolated by filtration, washed with deionized water and dried in an oven overnight at 333 K for 12 h.

12. Synthesis of 1.0% Au-CdS NWs nanocomposite by $NaBH_4$ reduction method

Typically, CdS NWs (100 mg) was dissolved in 100 mL deionized water with in an ice bath followed by adding 50 μL of $HAuCl_4$ solution (40 mg/mL) into the abovementioned solution. After 60 min under magnetic stirring, 10 mL of freshly prepared $NaBH_4$ (40 mg) aqueous solution was added dropwise. The mixture was aged for 3 h at 273 K. The precipitate was then separated by filtration, washed with water and dried at 333 K for 12 h.

Results and discussion

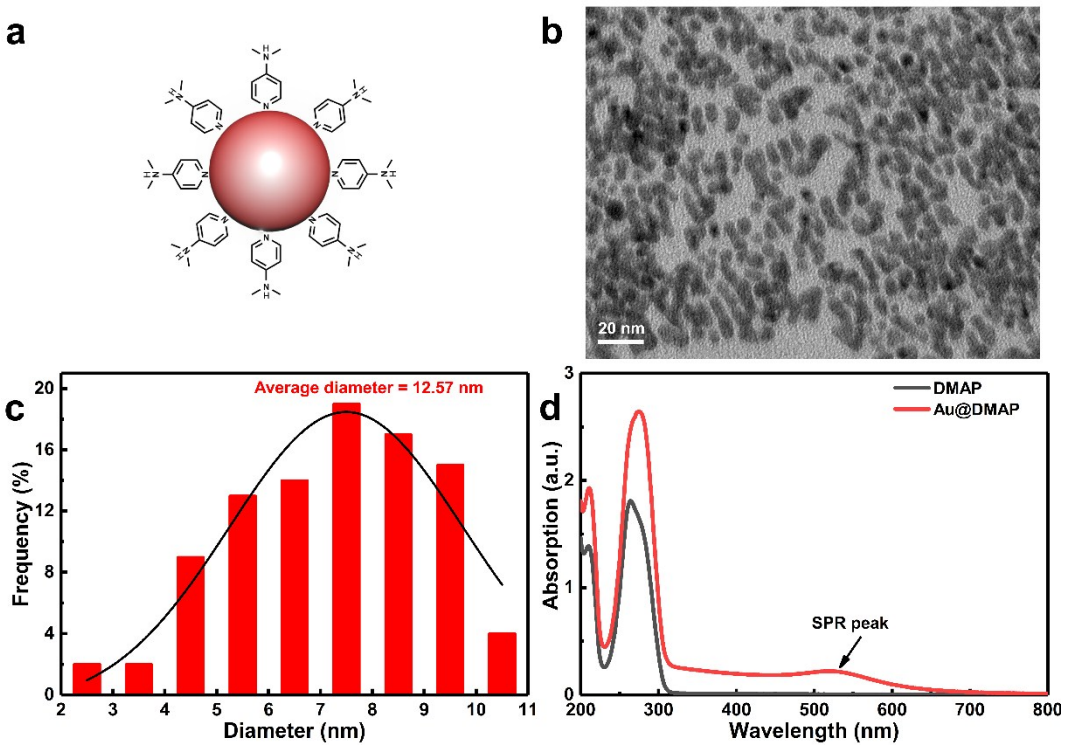

Fig. S1. (a) Specific molecule structure of DMAP ligand capped on the Au@DMAP NPs surface, (b) TEM image of Au@DMAP NPs with corresponding (c) size distribution histogram and (d) UV-vis absorption spectra of DMAP and Au@DMAP NPs colloidal solution.

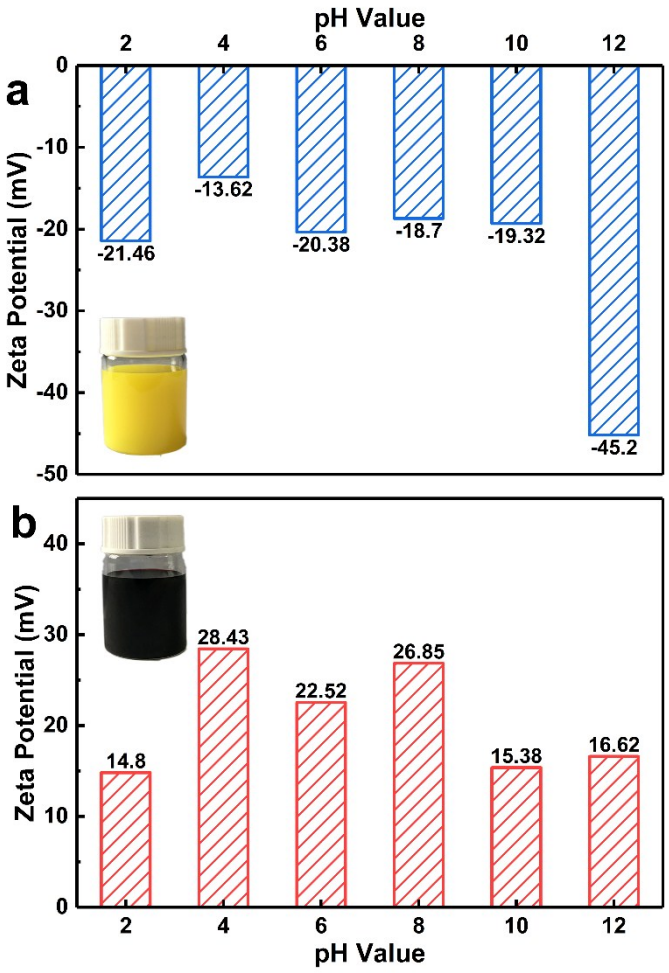

Fig. S2. Zeta potentials of (a) CdS@MAA NWs and (b) Au@DMAP NPs as a function of pH value.

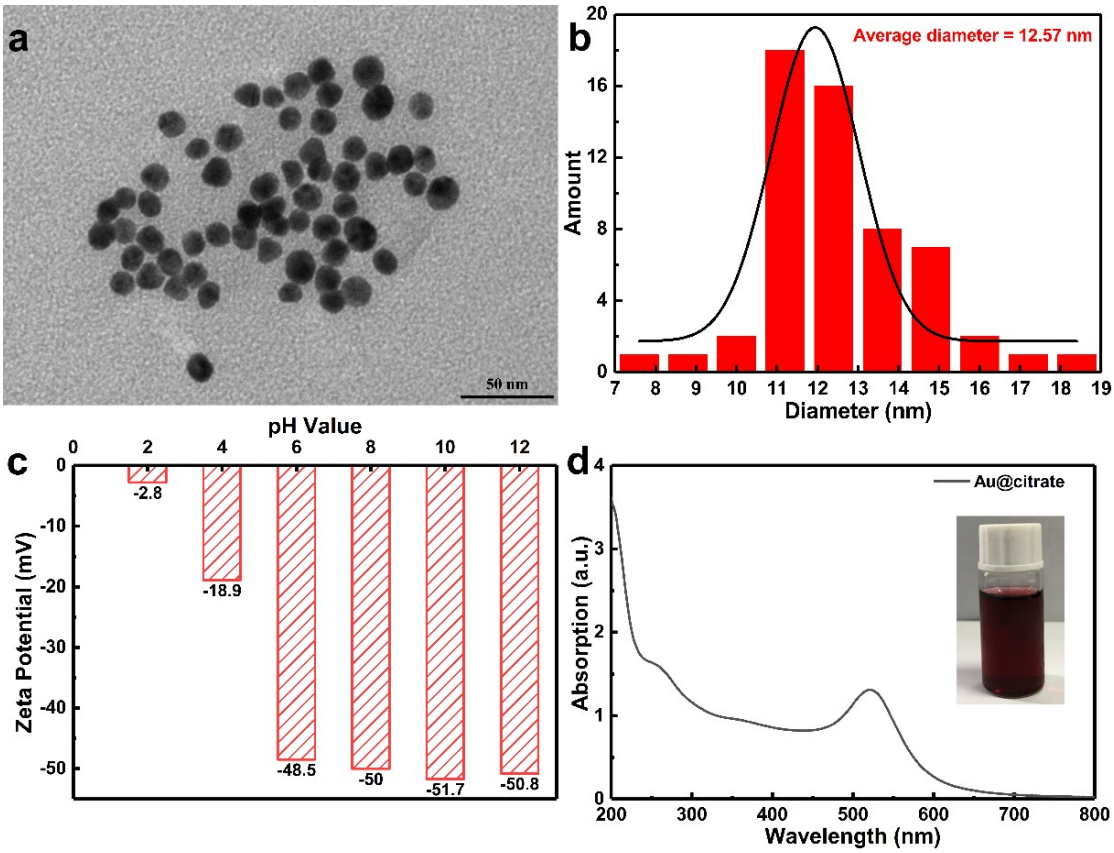

Fig. S3. (a) TEM image of Au@citrate NPs with corresponding (b) size distribution histogram, (c) zeta potentials of Au@citrate NPs as a function of pH value and (d) UV-vis absorption spectrum of Au@citrate NPs colloidal solution.

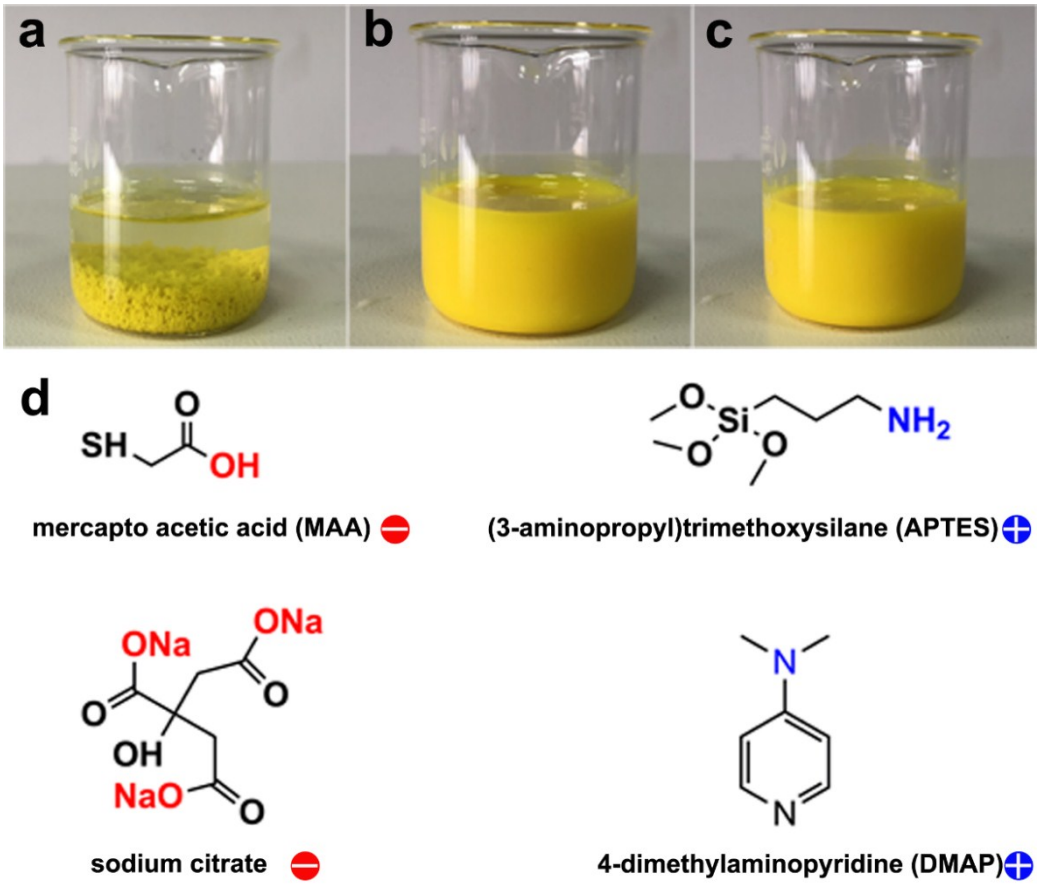

Fig. S4. Photographs of (a) Au@DMAP-CdS@MAA NWs and (b) Au@citrate-CdS@MAA NWs aqueous suspensions by adding positively charged Au@DMAP NPs and negatively charged Au@citrate NPs aqueous solution dropwise into negatively charged CdS@MAA NWs aqueous dispersion with vigorous stirring for 2 h; (c) Photograph of Au@DMAP-CdS@APTES NWs by adding positively charged Au@DMAP NPs aqueous solution dropwise into positively charged CdS@APTES NWs aqueous dispersion with vigorous stirring for 2 h; (d) Molecular structures of different ligands and surface charge mediators.

Note: Ligand-stabilized Au aqueous solutions including Au@DMAP NPs and Au@citrate NPs were separately added dropwise into CdS@MAA NWs aqueous solution under vigorous stirring for the same time (2 h) to trigger the spontaneous self-assembly. Obviously, positively charged Au@DMAP NPs can be spontaneously and rapidly deposited on the negatively charged CdS@MAA NWs matrix due to strong electrostatic attraction. Contrarily, negatively charged Au@citrate NPs cannot be deposited on the CdS@MAA NWs by virtue of the substantial electrostatic repulsion between them. Consistently, as reflected by **Fig. S4 (a & b)**, no sediment was observed when Au@citrate NPs aqueous suspension was added into the CdS@MAA NWs solution, which is remarkably different to the phenomenon observed by adding Au@DMAP NPs into the CdS@MAA NWs solution. Similar phenomenon was observed when positively charged Au@DMAP NPs were dropwise added into positively charged CdS@APTES NWs aqueous dispersion (**Fig. S4c**). Thus, control experiments strongly indicate that inherent surface charge properties of Au@DMAP NPs play a crucial role in triggering the electrostatic self-assembly of Au-CdS NWs heterostructures.

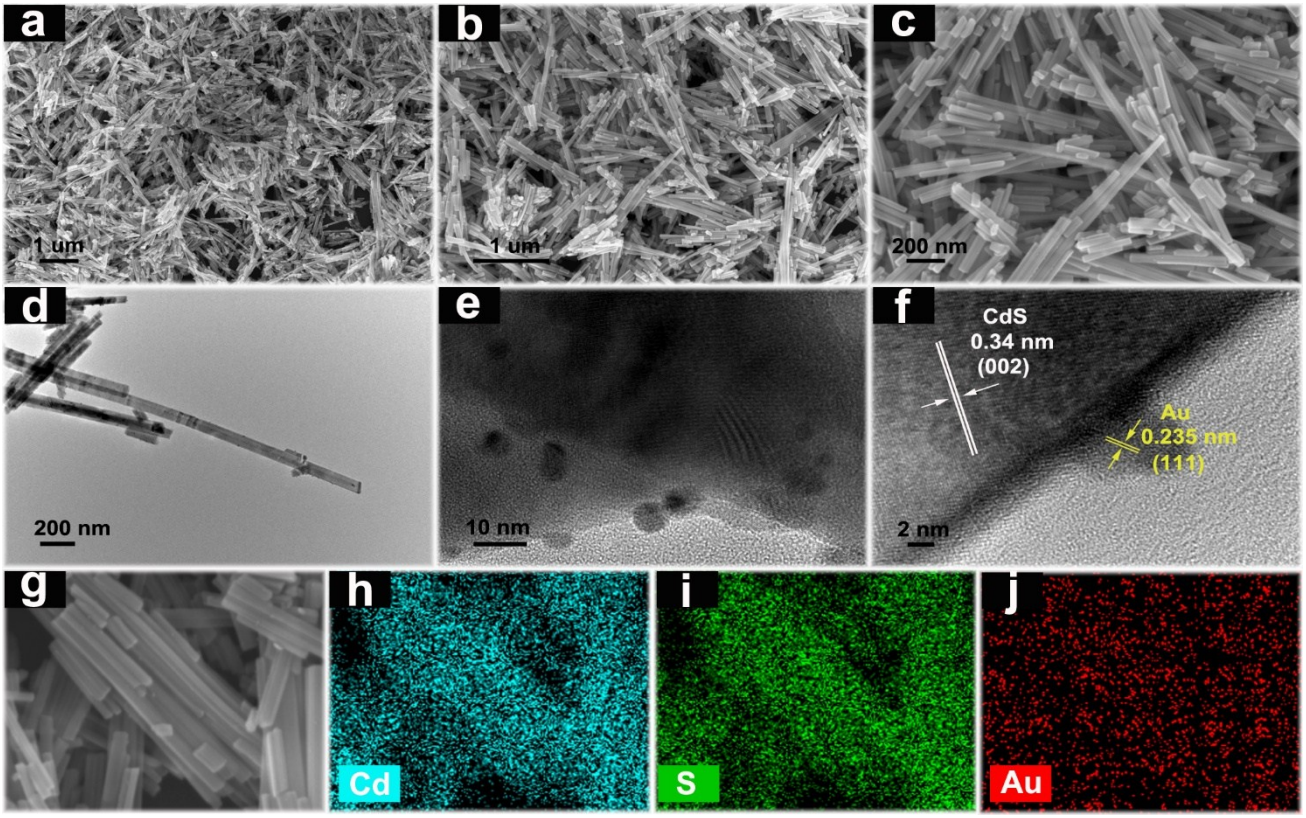

Fig. S5. Panoramic FESEM images of (a) blank CdS NWs and (b & c) 1.0% Au-CdS NWs heterostructure; TEM images of (d) pristine CdS NWs and (e) 1.0% Au-CdS NWs heterostructure, (f) HRTEM image and (g-j) elemental mapping results of 1.0% Au-CdS NWs heterostructure.

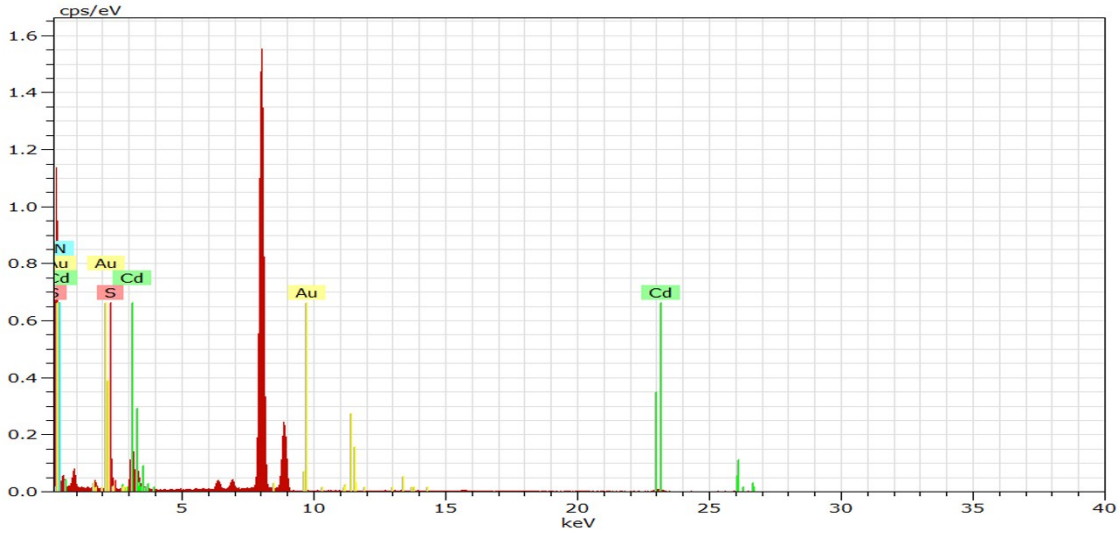

Fig. S6. EDS result of 1.0% Au-CdS NWs heterostructure.

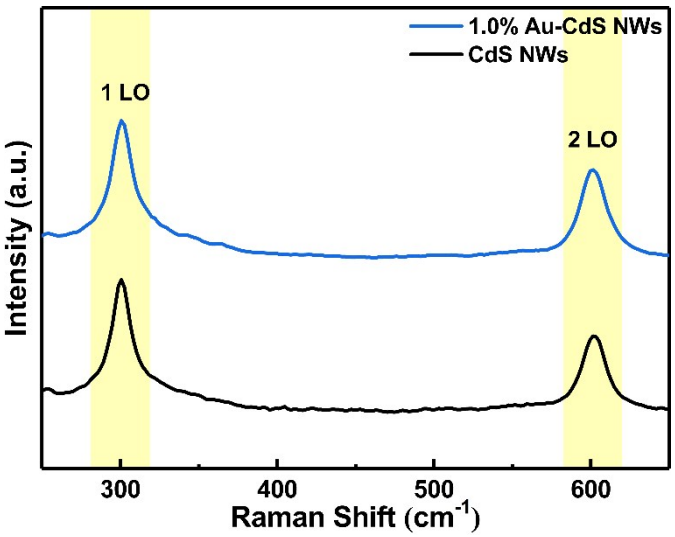

Fig. S7. Raman spectra of pristine CdS NWs and 1.0% Au-CdS NWs heterostructure.

Table S1. Chemical bond species vs. B.E. for different samples.

Elements	CdS NWs	1.0% Au-CdS NWs	Chemical Bond Species
Cd $3d_{5/2}$	404.15	404.9	Cd^{2+}
Cd $3d_{3/2}$	410.9	411.7	Cd^{2+}
S $2p_{3/2}$	160.55	161.3	S^{2-}
S $2p_{1/2}$	161.70	162.6	S^{2-}
Au $4f_{7/2}$	N.D.	83.98	Au^{0}
Au $4f_{5/2}$	N.D.	87.33	Au^{0}

N.D.: Not Detected

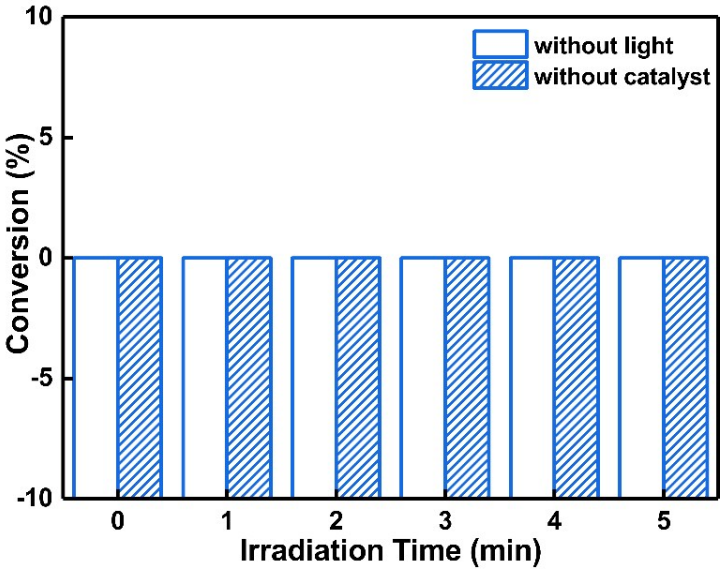

Fig. S8. Blank experiments for photocatalytic reduction of 4-NA without light irradiation or without adding photocatalyst.

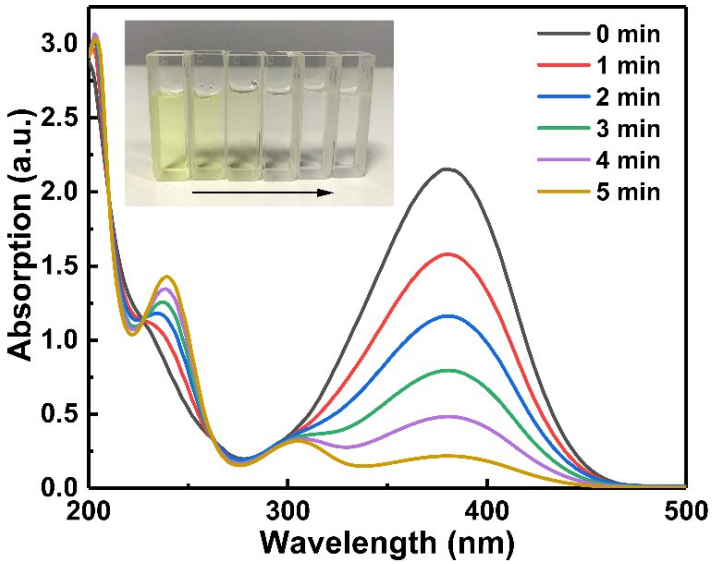

Fig. S9. UV-vis absorption spectra of 4-NA collected after designated irradiation time (1 min) when it was photoreduced over 1.0% Au-CdS NWs heterostructure under visible light irradiation (λ>420 nm) with the addition of ammonium formate as hole quencher and N_2 purge under ambient conditions.

Note: Absorption at 380 nm decreases and concomitantly, absorption at 240 nm and 300 nm increases, which implies gradual photoreduction of 4-NA to 4-PDA under visible light irradiation.[S1, 7]

Table S2. Photoreduction reaction rate constants (k) of different samples.

Substrate	CdS NWs	1.0% Au-CdS NWs	1.0% Au-CdS NWs (calcination)	1.0% Au-CdS NWs (PSS)
4-NA	0.034	0.399	0.566	0.229
2-NA	0.003	0.118	0.154	0.031
3-NA	0.006	0.075	0.091	0.034
2-NP	0.019	0.143	0.167	0.064
3-NP	0.007	0.151	0.175	0.045
4-NP	0.056	0.274	0.523	0.073
4-NT	0.047	0.292	0.389	0.226
1-chloro-4-nitrobenzene	0.037	0.287	0.875	0.264
1-bromo-4-nitrobenzene	0.226	0.308	0.369	0.241

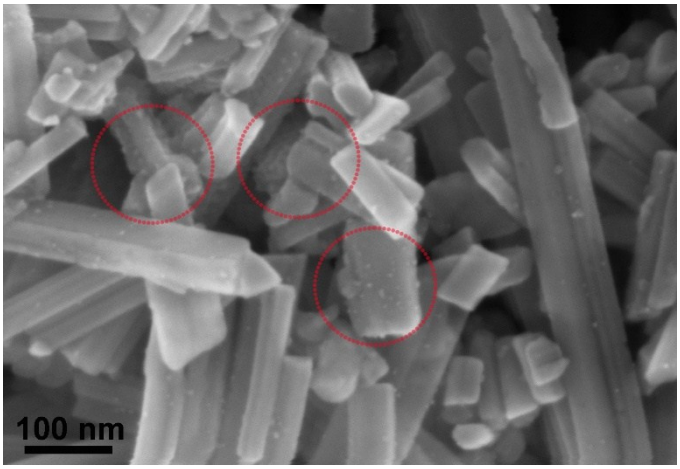

Fig. S10. FESEM image of 2.0% Au-CdS NWs.

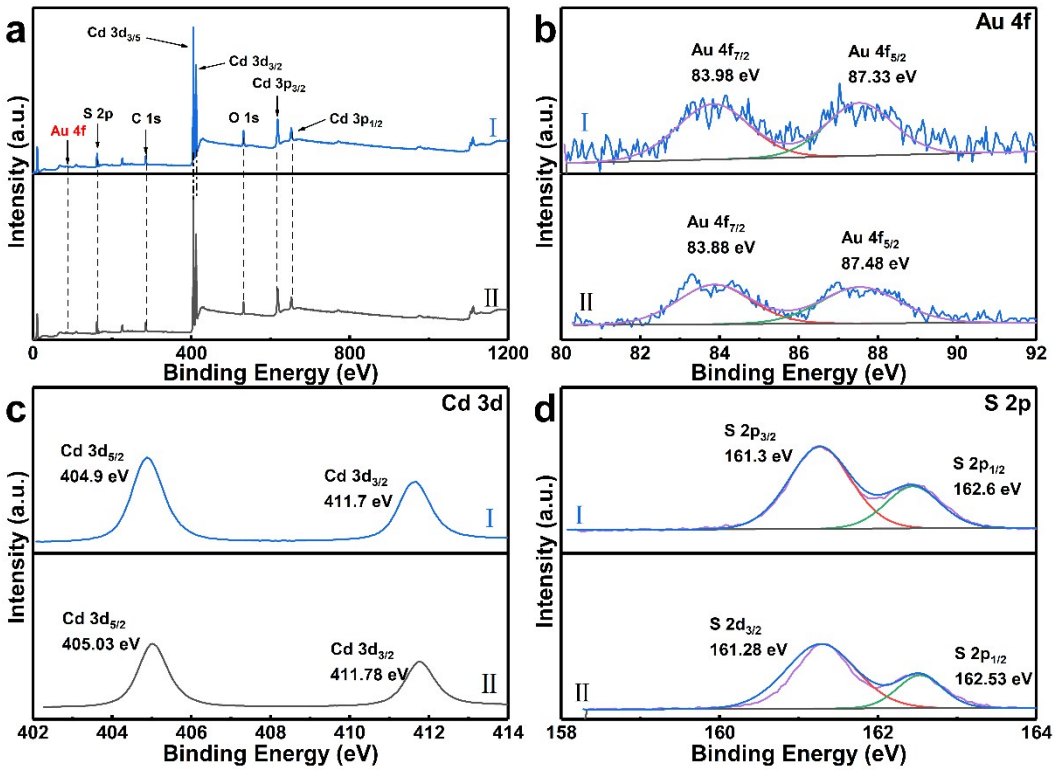

Fig. S11. Survey and high-resolution Cd 3d, S 2p and Au 4f spectra of 1.0% Au-CdS NWs heterostructure (I) before and (II) after cyclic photoreduction reactions.

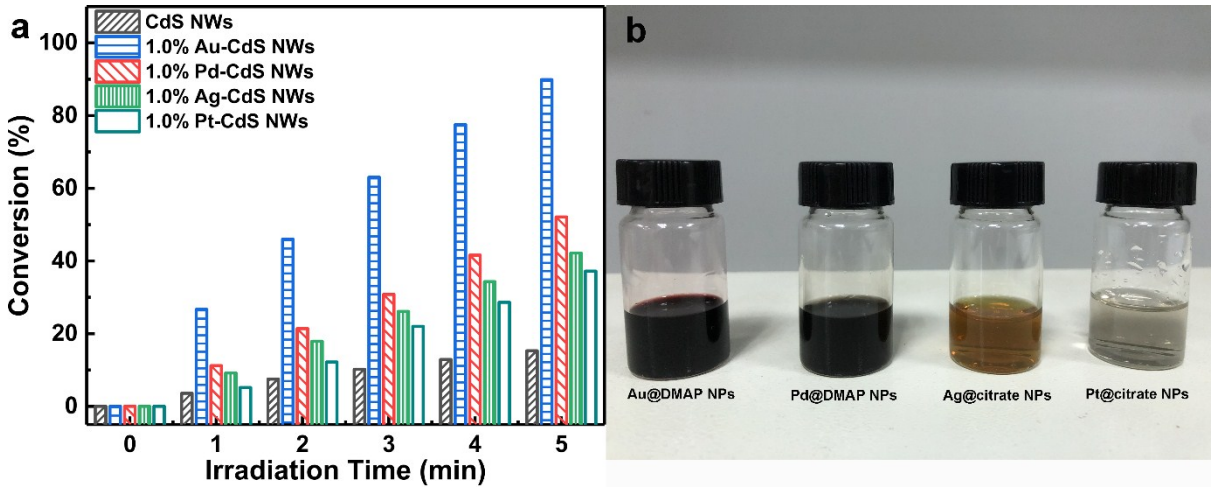

Fig. S12. (a) Photocatalytic activities of 1.0% M-CdS NWs (M = Au, Ag, Pt, Pd) toward 4-NA reduction under the same conditions. (b) Photographs of different metal NPs.

Note: 1.0% Pd-CdS NWs was prepared by same self-assembly strategy to 1.0% Au-CdS NWs other than replacing $HAuCl_4 \cdot 3H_2O$ precursor with Na_2PdCl_4 under the same experimental conditions. 1.0% Ag-CdS NWs and 1.0% Pt-CdS NWs were prepared by another electrostatic self-assembly strategy, wherein negatively charged citrate-stabilized Ag NPs & Pt NPs and positively charged APTES-modified CdS NWs were utilized as the building blocks.

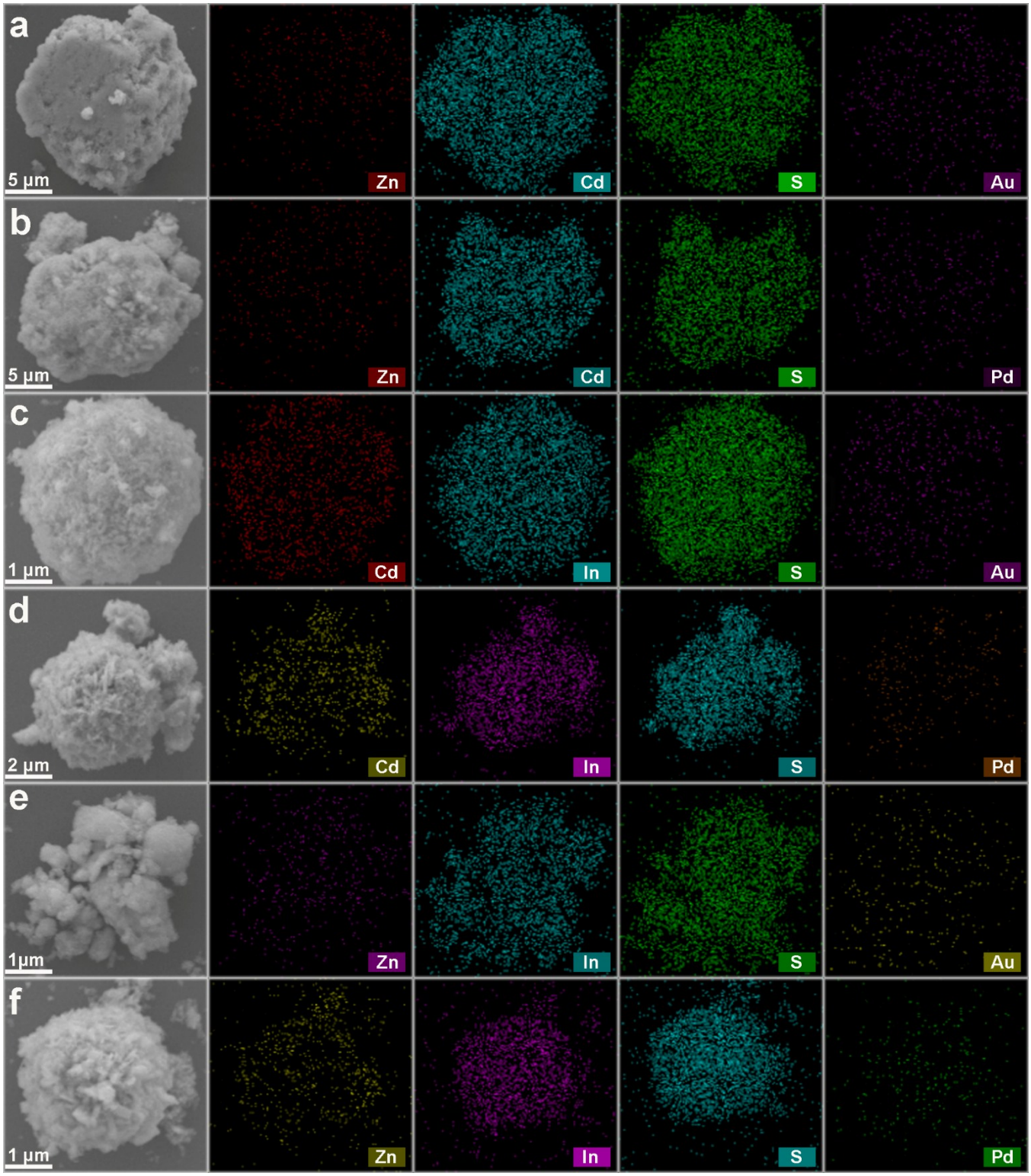

Fig. S13. Elemental mapping results of metal NCs (Au@DMAP, Pd@DMAP)/TMC ($Zn_{0.5}Cd_{0.5}S$, $CdIn_2S_4$, $ZnIn_2S_4$) heterostructures: (a) Au-$Zn_{0.5}Cd_{0.5}S$, (b) Pd-$Zn_{0.5}Cd_{0.5}S$, (c) Au-$CdIn_2S_4$, (d) Pd-$CdIn_2S_4$, (e) Au-$ZnIn_2S_4$ and (f) Pd-$ZnIn_2S_4$.

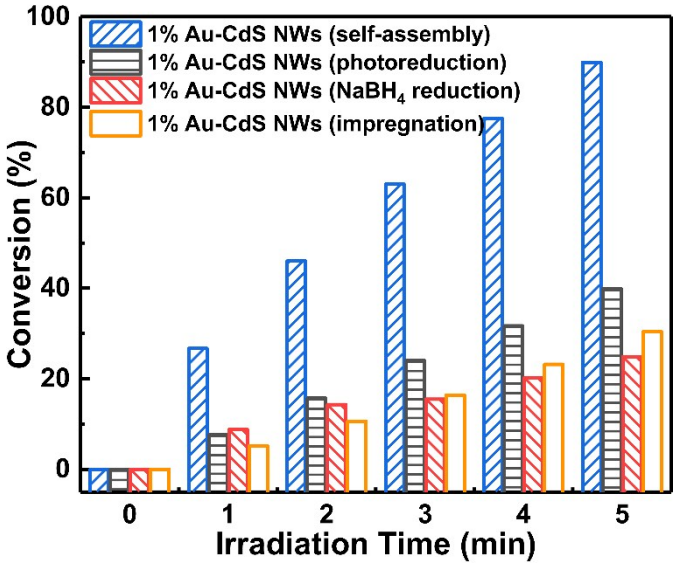

Fig. S14. Photoactivities of 1.0% Au-CdS NWs prepared by different methods toward 4-NA reduction under the same conditions.

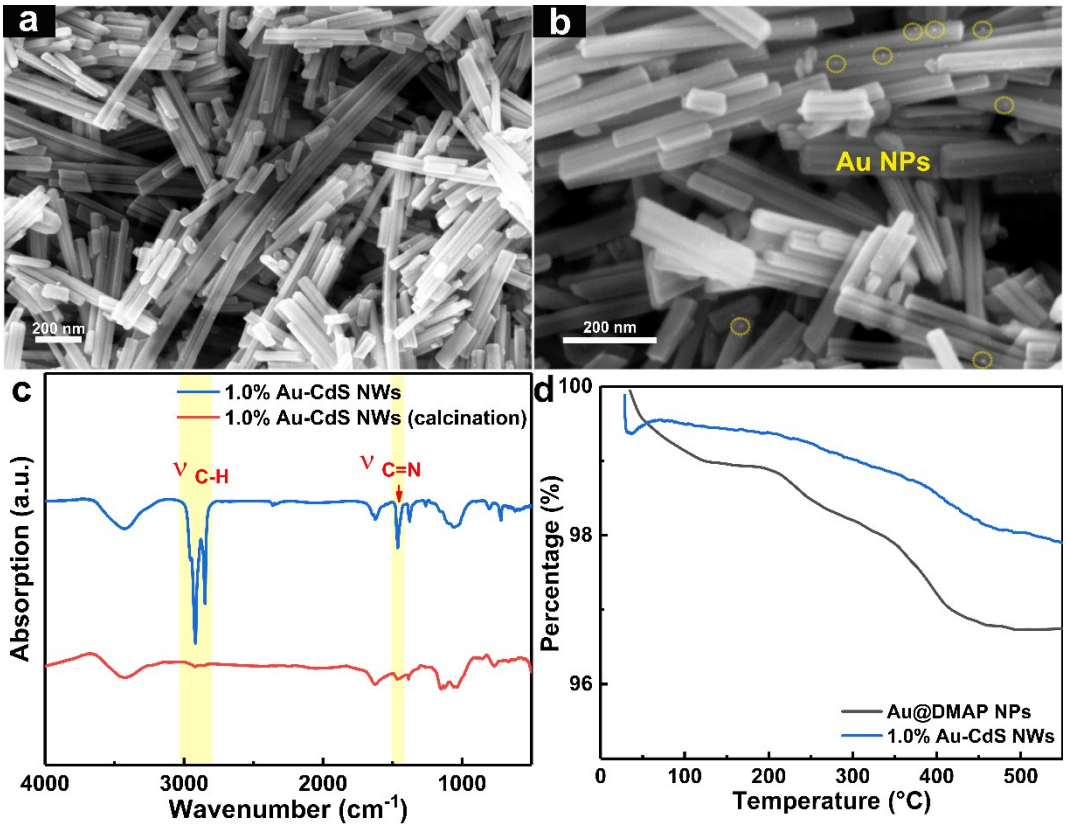

Fig. S15. (a) Low and (b) high-magnified FESEM images of 1.0% Au-CdS NWs after calcination in N_2 atmosphere (250 ℃), (c) FTIR spectra of pristine 1.0% Au-CdS NWs and calcined 1.0% Au-CdS NWs. (d) TGA curves of Au@DMAP NPs and 1.0% Au-CdS NWs.

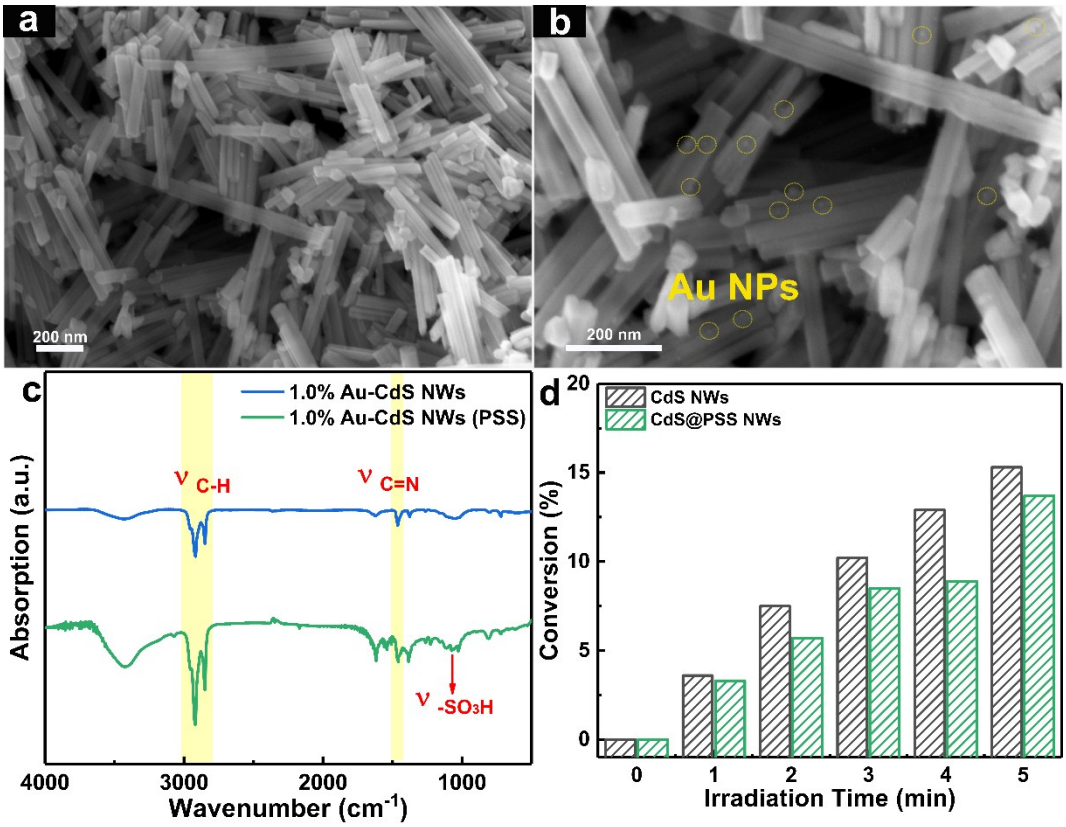

Fig. S16. (a) Low and (b) high-magnified FESEM images of 1.0% Au-CdS NWs (PSS) heterostructure prepared by utilizing CdS@PSS and Au@DMAP NPs as the building blocks, (c) FTIR spectra of pristine 1.0% Au-CdS NWs and 1.0% Au-CdS NWs (PSS), and (d) photoactivities of pure CdS NWs and CdS@PSS NWs toward 4-NA photoreduction under the same experimental conditions.

Note: The peak at 1078 cm^{-1} in the FTIR spectrum of 1.0% Au-CdS NWs (PSS) is assigned to the stretching vibration mode of sulfuric acid group ($-SO_3H$) from PSS ligand capped on the CdS NWs surface. Moreover, it is apparent that peak intensity at 2923 and 2852 cm^{-1} arising from PSS in the FTIR spectrum of 1.0% Au-CdS NWs (PSS) is more substantial than that in the FTIR spectrum of 1.0% Au-CdS NWs. The results strongly verify successful deposition of Au@DMAP NPs on the CdS@PSS NWs substrate via electrostatic interaction. Moreover, photoactivity of CdS@PSS toward 4-NA reduction under the same conditions was probed. As shown in **Fig. S16d**, photoactivity of CdS NWs is decreased after PSS encapsulation, suggesting the access of ammonium formate to CdS is indeed blocked to some extent with the involvement of PSS and the elimination of holes was slowed down, thus reducing the charge separation and slowing down the photoreduction of 4-NA. Nonetheless, it is worth noting that although the photoactivity of the CdS@PSS was inferior to blank CdS, the decremental value was rather limited, i.e., 13.7%. Therefore, the effect of PSS on the intrinsic photocatalytic performance of CdS can be ignored.

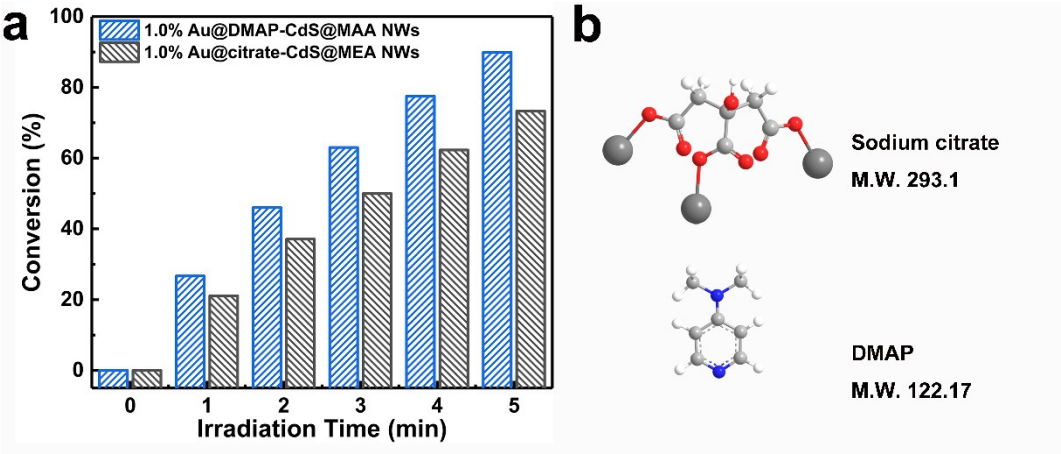

Fig. S17. Photoreduction performance of 1.0% Au-CdS NWs heterostructure by replacing DMAP with sodium citrate and replacing MAA with MEA.

Note: Another electrostatic self-assembly strategy was developed to fabricate Au-CdS nanocomposite for reasonable comparison, wherein negatively charged citrate-stabilized Au NPs (Au@citrate) and positively charged 2-mercaptoethylamine-modified CdS NWs (CdS@MEA) were utilized as the building blocks. Photoactivity of 1.0% Au@citrate-CdS@MEA NWs toward 4-NA reduction under the same conditions was provided in **Fig. S17a**, from which it is apparent that photoactivity of 1.0% Au@citrate-CdS@MEA NWs is lower than original 1.0% Au@DMAP-CdS@MAA NWs, owing probably to the steric effect caused by the long molecular chain of sodium citrate considering the similar structures of MAA and MEA (**Fig. S17b**).

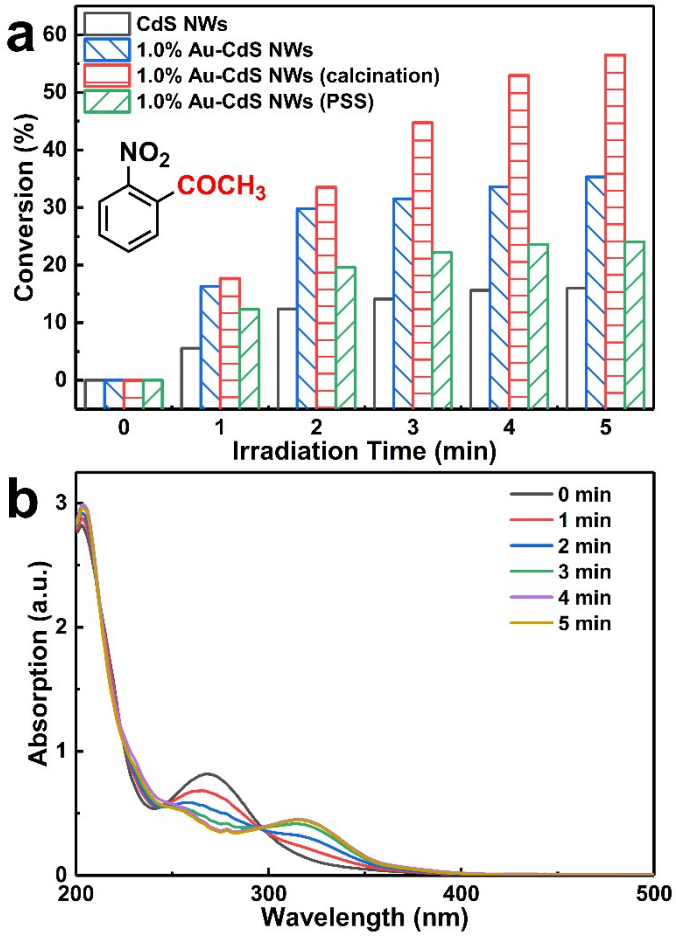

Fig. S18. (a) Photoactivities of different samples toward selective reduction of o-nitroacetophenone under visible light irradiation (λ>420 nm) with the addition of ammonium formate as hole scavenger and N_2 bubbling at ambient conditions. (b) UV-vis absorption spectra of o-nitroacetophenone collected after designated irradiation time (1 min) when it was photoreduced over 1.0% Au-CdS NWs heterostructure

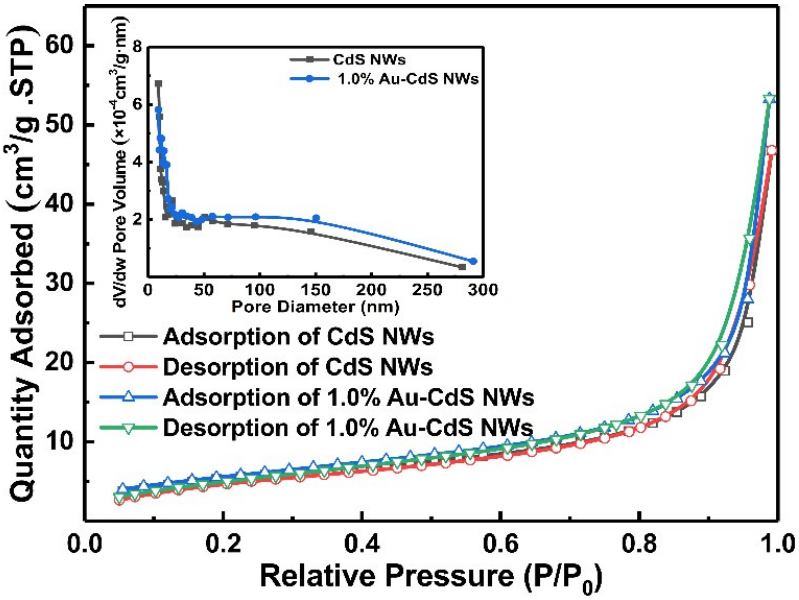

Fig. S19. Nitrogen adsorption-desorption isotherms of blank CdS NWs and 1.0% Au-CdS NWs heterostructure with corresponding pore size distribution plots in the inset.

Table S3. Specific surface area, pore volume and pore size of blank CdS NWs and 1.0% Au-CdS NWs heterostructure.

Samples	S_{BET} *(m² /g)* [a]	*Total pore volume (cm³ /g)* [b]	*Average pore size (nm)* [c]
CdS NWs	19.5493	0.071526	6.86537
1.0% Au-CdS NWs	20.6210	0.082126	7.22796

[a] BET surface area is calculated from the linear part of BET plots.
[b] Single point total pore volume of the pores at $P/P_0 = 0.99$.
[c] Adsorption average pore width (4V/A by BET).

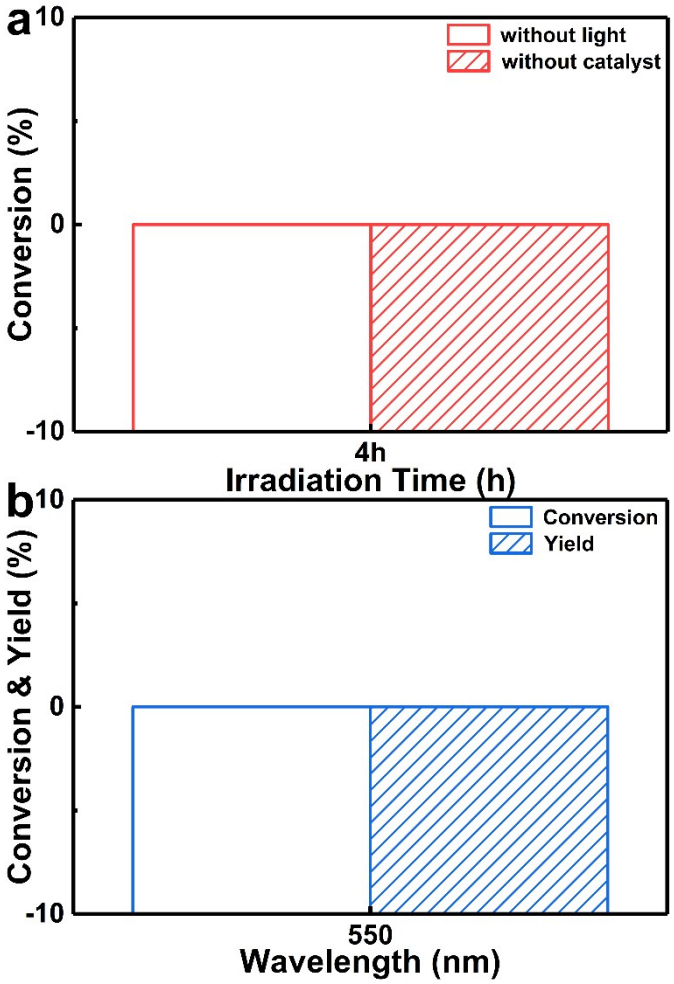

Fig. S20. (a) Blank experiments for photocatalytic selective oxidation of benzyl alcohol without light irradiation or without adding photocatalyst and (b) photoactivity of 1.0% Au-CdS NWs toward selective oxidation of benzyl alcohol under monochromatic light irradiation with a wavelength of 550 nm.

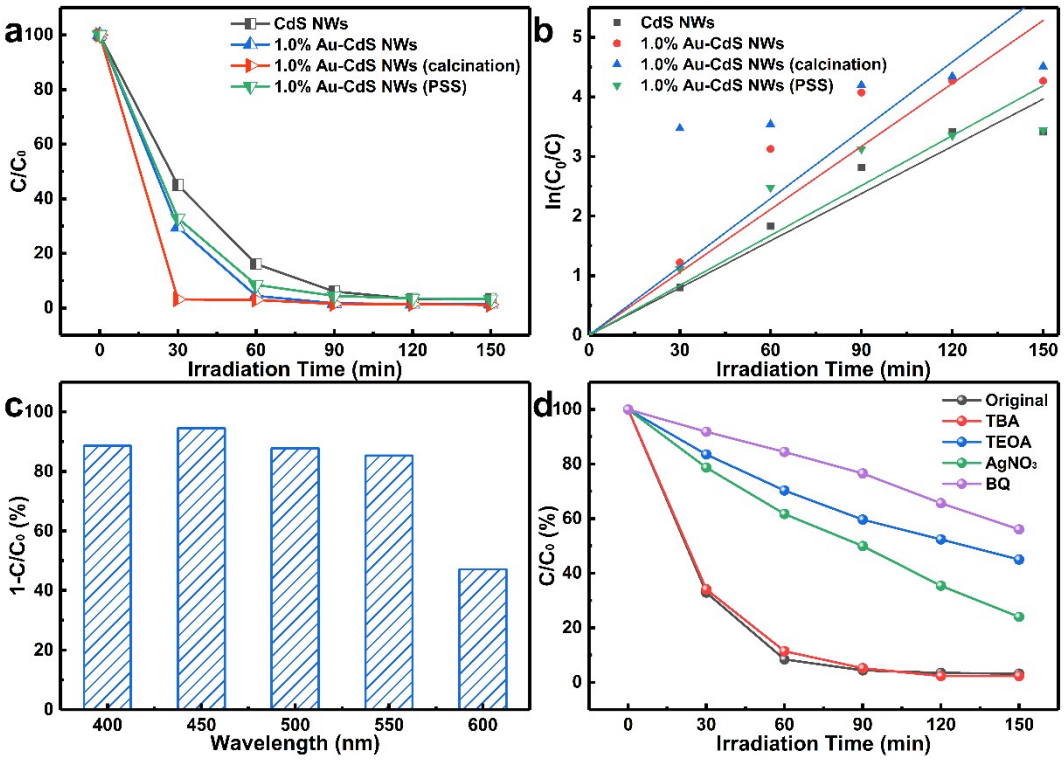

Fig. S21. (a) Photoactivities of blank CdS NWs, 1.0% Au-CdS NWs, calcined 1.0% Au-CdS NWs and 1.0% Au-CdS NWs (PSS) toward mineralization of RhB under visible light irradiation (λ>420 nm) with corresponding kinetic fitting curves displayed in (b), (c) cyclic photocatalytic reactions of 1.0% Au-CdS NWs and (d) photocatalytic performances of 1.0% Au-CdS NWs by adding BQ, TBA, TEOA and $AgNO_3$ in the reaction system as scavengers for quenching superoxide radicals ($O_2^{\bullet-}$), hydroxyl radicals ($OH^{\bullet}$), hole (h^+) and electrons (e^-), respectively.

Note: To gain more deep understanding on the universal role of Au@DMAP NPs in modulating the interfacial charge transfer, photocatalytic mineralization of Rhodamine B (RhB) was carried out. Apparently, as shown in **Fig. S21 (a & b)**, RhB molecules were completely degraded after visible light irradiation for 30 min over calcined 1.0%Au-CdS NWs which demonstrates the optimal photoactivity among different samples and the result is in line with other photoredox and PEC performances. Additionally, action spectrum of 1.0% Au-CdS NWs under different monochromatic light irradiation was probed to determine whether the SPR effect of Au NPs is responsible for the photocatalytic degradation of RhB. **Fig. S21c** manifests that no obvious SPR peak is observed in the action spectra within the wavelength profile of 500-600 nm and the result persuasively eliminates the SPR effect of Au NPs on enhancing the photoactivity of 1.0%Au-CdS NWs. Moreover, control experiments by adding BQ, TEOA and $AgNO_3$ in the reaction system suggest the primarily active species involved in the photooxidation reaction are $O_2^{\bullet-}$, holes, and electrons, whereas $OH^{\bullet}$ radicals exert negligible influence on the photoactivity of Au-CdS NWs.

References

1. S. Liu and Y.-J. Xu, *Nanoscale*, 2013, **5**, 9330-9339.
2. Q. Nie, Q. Yuan, Q. Wang and Z. Xu, *J. Mater. Sci.*, 2004, **39**, 5611-5612.
3. J. Q. Hu, B. Deng, W. X. Zhang, K. B. Tang and Y. T. Qian, *Inorg. Chem.*, 2001, **40**, 3130-3133.
4. X. Gou, F. Cheng, Y. Shi, L. Zhang, S. Peng, J. Chen and P. Shen, *J. Am. Chem. Soc.*, 2006, **128**, 7222-7229.
5. D. I. Gittins and F. Caruso, *Angew. Chem. Int. Edit.*, 2001, **40**, 3001-3004.
6. D. M. Dotzauer, J. Dai, L. Sun and M. L. Bruening, *Nano Lett.*, 2006, **6**, 2268-2272.
7. Q. Xu, J. Zeng, H. Wang, X. Li, J. Xu, J. Wu, G. Xiao, F.-X. Xiao and X. Liu, *Nanoscale*, 2016, **8**, 19161-19173.